THE JOURNAL OF BIOLOGICAL CHEMISTRY VOL. 288, NO. 25, pp. 18521–18532, June 21, 2013

A New Class of Endoplasmic Reticulum Export Signal ΦXΦXΦ for Transmembrane Proteins and Its Selective Interaction with Sec24C*[S]

Received for publication, December 7, 2012, and in revised form, April 24, 2013 Published, JBC Papers in Press, May 8, 2013, DOI 10.1074/jbc.M112.443325

Wataru Otsu[1], **Takao Kurooka**[2], **Yayoi Otsuka, Kota Sato, and Mutsumi Inaba**[3]

From the Laboratory of Molecular Medicine, Department of Veterinary Clinical Sciences, Graduate School of Veterinary Medicine, Hokkaido University, Sapporo 060-0818, Japan

Background: Endoplasmic reticulum (ER) export of transmembrane proteins depends on the interaction between cargo signals and Sec24 isoforms.
Results: The ΦXΦXΦ sequence facilitates the ER export of model proteins and selectively binds to Sec24C.
Conclusion: ΦXΦXΦ is a novel ER export signal that is specifically recognized by Sec24C.
Significance: This novel cargo-Sec24 interaction provides mechanistic insights into vesicular transport.

Protein export from the endoplasmic reticulum (ER) depends on the interaction between a signal motif on the cargo and a cargo recognition site on the coatomer protein complex II. A hydrophobic sequence in the N terminus of the bovine anion exchanger 1 (AE1) anion exchanger facilitated the ER export of human AE1Δ11, an ER-retained AE1 mutant, through interaction with a specific Sec24 isoform. The cell surface expression and *N*-glycan processing of various substitution mutants or chimeras of human and bovine AE1 proteins and their Δ11 mutants in HEK293 cells were examined. The N-terminal sequence (V/L/F)*X*(I/L)*X*(M/L), ^{26}VSIPM^{30} in bovine AE1, which is comparable with ΦXΦXΦ, acted as the ER export signal for AE1 and AE1Δ11 (Φ is a hydrophobic amino acid, and *X* is any amino acid). The AE1-Ly49E chimeric protein possessing the ΦXΦXΦ motif exhibited effective cell surface expression and *N*-glycan maturation via the coatomer protein complex II pathway, whereas a chimera lacking this motif was retained in the ER. A synthetic polypeptide containing the N terminus of bovine AE1 bound the Sec23A-Sec24C complex through a selective interaction with Sec24C. Co-transfection of Sec24C-AAA, in which the residues ^{895}LIL^{897} (the binding site for another ER export signal motif I*X*M on Sec24C and Sec24D) were mutated to ^{895}AAA^{897}, specifically increased ER retention of the AE1-Ly49E chimera. These findings demonstrate that the ΦXΦXΦ sequence functions as a novel signal motif for the ER export of cargo proteins through an exclusive interaction with Sec24C.

Export from the endoplasmic reticulum (ER)[4] is the first sorting event in the vesicular transport of membrane proteins to their final destinations in the cell. In general, selective export from the ER depends on the interaction between an export signal motif in the cytoplasmic regions of the cargo and a cargo recognition site on the coatomer protein complex II (COPII) coat (1–3). Several ER export motifs have been identified, and diacidic (D/E)*X*(D/E) and dihydrophobic (FF, LL, VV, etc.) motifs have been well characterized. Diacidic motifs have been identified in several transmembrane proteins including vesicular stomatitis virus glycoprotein (VSV-G) (4), cystic fibrosis transmembrane conductance regulator (5), and some inwardly rectifying potassium channels (6). Dihydrophobic motifs are required for the ER export of ERGIC53 (7, 8). Moreover, the L*XX*LE motif of the yeast SNARE protein Bet1 (9, 10); the I*X*M motif of the SNARE proteins, membrin, and syntaxin 5 (11); and the RI/RL motifs in serotonin and GABA transporters are ER export codes (12, 13).

COPII-coated vesicles comprise three principal components, Sar1-GTP, Sec23-Sec24, and Sec13-Sec31 protein complexes, which function in concert to promote budding of vesicles for transport (2, 14–16). Sec24 is the primary cargo selection element of the coat (1, 9, 10). In mammals, the presence of multiple Sec24 isoforms (A–D), with at least four cargo binding sites on each isoform, means that there are a number of ER export signals to which Sec24 can bind and that the range and specificity of cargo-Sec24 interactions is diverse (14–16). For example, dihydrophobic motifs bind to all four Sec24 isoforms with varying strength (17). Although the L*XX*LE and D*X*E classes of signals selectively bind to Sec24A-Sec24B, the I*X*M sequence specifically binds to the surface groove on Sec24C-Sec24D, which is occluded in Sec24A-Sec24B (11). Furthermore, there are several examples in which a single iso-

* This work was supported by Grants-in-Aid for Scientific Research 19208027, 22658095, and 23658257 (to M. I.) from the Japan Society for the Promotion of Science.
[S] This article contains supplemental Tables S1 and S2.
[1] Supported by a Research Fellowship for Young Scientist from Japan Society for the Promotion of Science.
[2] Present address: Safety Research Laboratory, R & D, Kissei Pharmaceutical Co. Ltd., Azumino, Nagano 399-8305, Japan.
[3] To whom correspondence should be addressed: Laboratory of Molecular Medicine, Graduate School of Veterinary Medicine, Hokkaido University, Sapporo 060-0818, Japan. Tel.: 81-11-706-5580; Fax: 81-11-706-5276; E-mail: inazo@vetmed.hokudai.ac.jp.

[4] The abbreviations used are: ER, endoplasmic reticulum; AE1, anion exchanger 1; AE1Δ11, erythroid AE1 lacking the 11 C-terminal amino acid residues; bAE1, bovine AE1; COPII, coatomer protein complex II; EGFP, enhanced green fluorescent protein; endo H, endoglycosidase H; hAE1, human AE1; kAE1, kidney AE1; VSV-G, vesicular stomatitis virus glycoprotein.

form is absolutely required; for example, Sec24C and Sec24D differentially mediate the ER export of the highly related neurotransmitter transporters of serotonin and GABA (12, 13). No human diseases resulting from genetic defects in Sec24 have been found to date; however, animal models of defects in some Sec24 isoforms, human diseases caused by the defects in other components of the COPII pathway (18), and a subtype of cystic fibrosis caused by a missense mutation of cystic fibrosis transmembrane conductance regulator at the diacidic ER export signal (5, 19) have been reported. It is conceivable that impairment of the cargo-Sec24 interaction can affect ER-Golgi transport and subsequent expression of membrane proteins in the appropriate compartments of the cell, thereby causing various disease phenotypes.

Anion exchanger 1 (AE1, also known as band 3) is expressed primarily in the plasma membrane of red blood cells and the intercalated cells of the renal collecting duct. AE1 is critical for the mechanical stabilization of the red cell membrane by linking the membrane skeleton to the lipid bilayer through association with the anchor protein ankyrin and in maintaining the acid-base balance through rapid Cl^-/HCO_3^- exchange across the membrane (20, 21). AE1 proteins in the kidney and red blood cells have different N-terminal structures. Human erythroid AE1 possesses an N-terminal stretch consisting of 65 amino acid residues (see Fig. 1*A*). Various mutations of the AE1 gene (*SCL4A1*) in humans and animals cause hereditary spherocytosis and distal renal tubular acidosis, which are dominantly inherited (21–23). Human kidney AE1 (kAE1) with a nonsense mutation at Arg^{901}, which truncates AE1 by 11 amino acid residues at the C terminus (kAE1Δ11), impairs the basolateral sorting of the protein in polarized epithelial cell lines. The conserved tyrosine-based Y*XX*Φ motif (*X* is any amino acid, and Φ is a hydrophobic amino acid), which corresponds to ^{904}YDEV^{907} in human erythroid AE1, is involved in the membrane trafficking of kAE1 to the basolateral membrane (24, 25) along with a tyrosine residue in the N-terminal cytoplasmic domain (26). Interestingly, kAE1Δ11 is retained in the ER in nonpolarized MDCK (25, 27) and HEK293 cells (28). The ^{904}YDEV^{907} sequence is not necessary for the plasma membrane targeting of erythroid AE1, because the AE1 content in red blood cells from patients with the Δ11 mutation is only mildly reduced (27).

During a series of studies on the mechanism(s) underlying the ER quality control of the AE1 mutant (22, 29), we found that the highly conserved C-terminal EL*XX*L(D/E) sequence, which conforms to the L*XX*LE class motif, is essential for efficient expression of AE1 at the plasma membrane in transfected HEK293 cells (30). We also showed that bovine and murine erythroid AE1 lacking the C-terminal Y*XX*Φ motif (AE1Δ11) are successfully transported to the plasma membrane, whereas human erythroid AE1Δ11 is retained in the ER (28). These findings suggest that AE1 in nonpolarized cells (erythroid and HEK293) and polarized cells (renal epithelial and polarized MDCK) have different signals for ER exit and/or that AE1 proteins from different species use distinct codes for ER export. However, the mechanism responsible for ER export, including the selectivity of AE1 for the COPII machinery, remains unknown.

In the present study, we examined the signal motif responsible for the ER export and efficient plasma membrane expression of bovine erythroid AE1 (bAE1). We analyzed the intracellular transport of a series of AE1 mutants and chimeric proteins of AE1 and Ly49E. Ly49E is a type II transmembrane protein that is expressed in natural killer cells of fetal mice and is a member of the Ly49 receptor family, which recognizes MHC class I molecules (31, 32). A hydrophobic cluster resembling a Φ*X*Φ*X*Φ sequence in the N-terminal stretch of bAE1 significantly increased the ER exit of AE1 and the AE1-Ly49E chimera through the COPII pathway, irrespective of whether the C-terminal Y*XX*Φ motif was absent or present. We demonstrate that the Φ*X*Φ*X*Φ motif exclusively interacts with Sec24C at the binding site for the L*X*M motif, which is also present in Sec24D (11), to facilitate ER-Golgi transport.

EXPERIMENTAL PROCEDURES

Antibodies—The antibodies used were: anti-GFP (MBL, Nagoya, Japan), anti-Myc (BD Biosciences Clontech), anti-calnexin (Stressgen, Victoria, Canada), anti-GM130 (BD Transduction Laboratories), and anti-Sec23 and anti-ERGIC53 (Sigma-Aldrich).

Construction of Plasmids—Plasmid vectors encoding N-terminally enhanced GFP (EGFP)-tagged bAE1 and bAE1Δ11 and mouse erythroid AE1 (pEGFP-bAE1, pEGFP-bAE1Δ11, and pEGFP-mAE1, respectively) were prepared as described previously (29, 30). Erythroid AE1 cDNAs for human, dog, and horse (GenBank™ accession numbers NM_00342, AB242565, and AB242566, respectively) were obtained by PCR amplification of cDNAs from K562 cells and bone marrow cells from healthy dogs and horses, respectively. The cDNA fragments for AE1 were subcloned into the pEGFP-C3 vector (BD Biosciences Clontech), and the Δ11 truncation mutants were generated by PCR using the appropriate primer pairs as described previously (30). The nucleotide sequences of the PCR primers used in the present study are shown in supplemental Table S1.

To prepare chimeric AE1 consisting of the bovine N-terminal cytoplasmic domain (amino acid residues 1–403) and the human C-terminal transmembrane domain with or without the Δ11 mutation (designated hAE1Δ11/b[1–403] and hAE1/b[1–403], respectively), we created the EcoRV site at the position corresponding to ^{403}DI^{404} by PCR without causing any amino acid substitutions. Then the cytoplasmic domain (residues 1–385) of hAE1 or hAE1Δ11 was replaced by the bovine sequence using the endogenous EcoRV site in the hAE1 sequence. Conversely, to make the construct for bAE1/h[1–385] or bAE1Δ11/h[1–385], the cDNA fragment encoding the bovine transmembrane domain was connected to the sequence encoding the cytoplasmic domain of hAE1 (or hAE1Δ11) using the EcoRV site. Similar procedures were employed to prepare plasmid vectors for a series of AE1 chimeras, except that the hAE1/b[25–29] and bAE1/h[26–31] vectors and their Δ11 forms were generated by PCR amplification using primers to introduce the appropriate amino acid substitutions (see Fig. 2). Likewise, vectors encoding a series of substitution mutants (see Fig. 3) were produced by PCR amplification using the appropriate mutagenic primers (supplemental Table S1).

cDNA containing the entire coding region of murine Ly49E (GenBank™ accession number NM_008463) was obtained by PCR amplification of whole cDNA obtained from a C57BL/6 mouse fetus and was inserted into the pEGFP-N3 vector (BD Biosciences Clontech). The cDNA fragment encoding the N-terminal cytoplasmic region of Ly49E was replaced by the 37 (bovine) or 39 (human) N-terminal amino acid residues of erythroid AE1 (bN[1–37] and hN[1–39], respectively) to create vectors encoding the AE1 N terminus-Ly49E chimeric protein that was C-terminally tagged with EGFP, namely bN[1–37]Ly, hN[1–39]Ly, and hN[P27V/S29I]Ly.

cDNA for the entire coding regions of human Sar1A, Sec24A, Sec24B, Sec24C, and Sec24D (GenBank™ accession numbers, NM_001142648, NM_021982, NM_006323, NM_004922, and NM_014822, respectively) were obtained by PCR amplification of HEK293 cell cDNA. Sar1A cDNA was elongated at the 3′ end using a primer containing the c-Myc epitope peptide (NH_2-QKLISEEDL-COOH) and subcloned into the pcDNA3.1 vector (Invitrogen). An activated GTP-bound form of Sar1A, Sar1A H79G (33), was generated by site-directed mutagenesis as described previously (29). The cDNA for each Sec24 isoform was cloned into the pCMV-Myc vector (BD Biosciences Clontech) to generate C-terminally Myc-tagged Sec24 proteins. Sec24C-AAA, in which the amino acid residues ^{895}LIL^{897} were mutated to ^{895}AAA^{897} (11), was generated by site-directed mutagenesis.

cDNA encoding VSV-G was obtained by PCR amplification of the pMD2.G vector (Addgene) and was subcloned into the pEGFP-N3 vector. Primers for these procedures are shown in supplemental Table S1. All experimental procedures met with the approval of the Laboratory Animal Experimentation Committee, Graduate School of Veterinary Medicine, Hokkaido University.

Cell Culture and Transfection—HEK293 cells were cultured and transfected with the appropriate plasmid vectors as previously described (29).

Analysis of Proteins—SDS-PAGE, immunoblotting, cell surface biotinylation, immunoprecipitation, and deglycosylation were performed as described previously (29, 30, 34). For biotinylation, the cells were washed with borate buffer (10 mM boric acid, 154 mM NaCl, 7.2 mM KCl, and 1.8 mM $CaCl_2$, pH 9.0) and were labeled with 0.8 mM sulfo-NHS-SS-biotin (Thermo Scientific) in the same buffer for 30 min at 4 °C. The cells were rinsed with PBS containing 1 mM $CaCl_2$, 1 mM $MgCl_2$, and 100 mM glycine to quench the reaction and lysed in radioimmune precipitation assay buffer containing 1% (w/v) deoxycholic acid, 1% (w/v) Triton X-100, 0.1% (w/v) SDS, 150 mM NaCl, 1 mM EDTA, and 10 mM Tris-HCl (pH 7.5). The cell lysate was centrifuged for 15 min at 20,000 × *g*, and the supernatant was incubated with NeutrAvidin beads (Thermo Scientific) for 1 h at 4 °C to capture the biotinylated proteins. After washing with radioimmune precipitation assay buffer, immobilized proteins were eluted in sample buffer for SDS-PAGE. For deglycosylation, proteins captured on the NeutrAvidin beads were incubated with or without endoglycosidase H (endo H) or peptide *N*-glycosidase F (both from Roche) in radioimmune precipitation assay buffer. After washing the beads once, the proteins were eluted in sample buffer for SDS-PAGE.

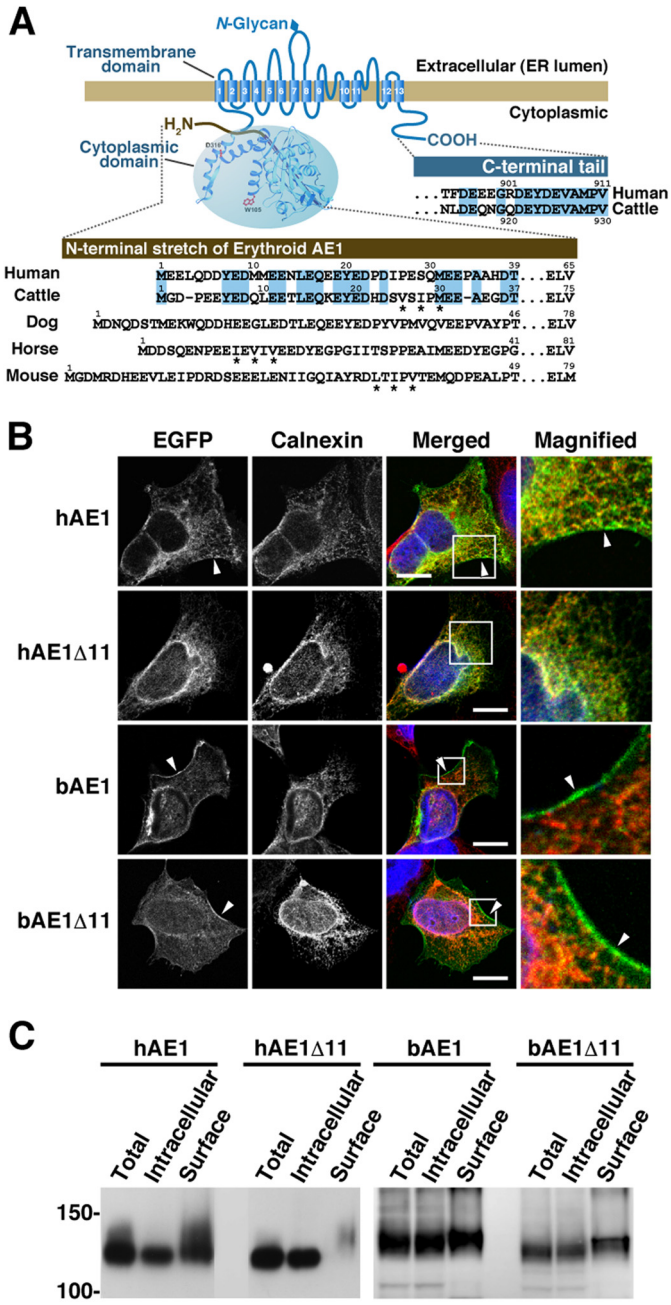

FIGURE 1. **Expression of human and bovine AE1 and their C-terminally truncated mutants in transfected HEK293 cells.** *A*, schematic illustration of erythroid AE1 based on the crystallographic structure of the cytoplasmic domain (36) and the topology model of the transmembrane domain (45). The amino acid sequences of the N- and C-terminal regions of human and bovine AE1 are aligned, and residues highlighted in *blue* are identical between humans and cattle. The N-terminal sequences of canine, equine, and murine AE1 are also shown. The N-terminal sequence varies between the species. The functions of these amino acid sequences in ER export were analyzed (Figs. 4–7), and *asterisks* indicate the hydrophobic residues that correspond to the ΦXΦXΦ motif. *B*, HEK293 cells were transfected with EGFP-tagged hAE1 or bAE1 and their C-terminally truncated mutants. The cells were fixed after 48 h, and EGFP and the ER marker calnexin were visualized. A merged image of EGFP- (*green*), calnexin- (*red*), and DAPI-stained nuclei (*blue*) is shown. The indicated areas in the merged images are magnified, and EGFP fluorescence at the plasma membrane is indicated by *arrowheads*. *Bars*, 10 μm. *C*, at 48 h after transfection, cell surface proteins were labeled with sulfo-NHS-SS-biotin. After solubilization, biotin-labeled proteins were separated from intracellular proteins on NeutrAvidin beads. AE1 proteins in total (*Total*), intracellular (*Intracellular*), and cell surface (*Surface*) fractions were detected by immunoblotting with an anti-GFP antibody. The amount of cell surface fraction loaded is 10-fold higher than that of the other fractions. Migrating positions of size markers are shown in kDa.

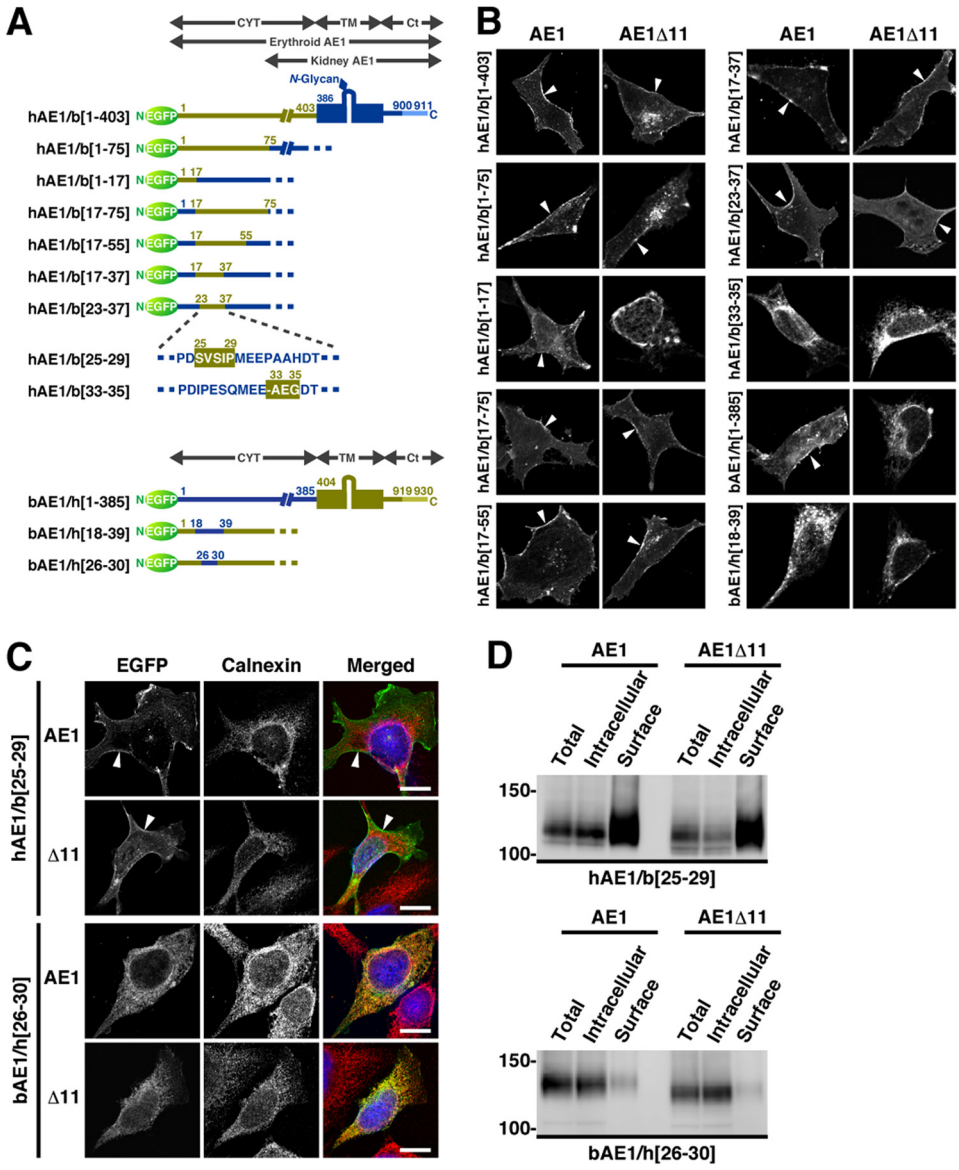

FIGURE 2. **Intracellular localization of a series of bAE1-hAE1 chimeric proteins and their Δ11 mutants.** *A*, a series of bAE1 and hAE1 chimeric proteins are schematically illustrated with the numbers of the amino acid residues shown. The overall structures of erythroid and kidney AE1 are presented along with a representative illustration of the hAE1/b[1–403] mutant. *CYT*, *TM*, and *Ct* indicate the cytoplasmic domain, the transmembrane domain, and the short C-terminal cytoplasmic tail, respectively. The chimeras hAE1/b[1–403], hAE1/b[1–75], hAE1/b[1–17], hAE1/b[17–75], hAE1/b[17–55], hAE1/b[17–37], hAE1/b[23–37], hAE1/b[25–29], and hAE1/b[33–35] have a hAE1 backbone and contain amino acid residues 1–403, 1–75, 1–17, 17–75, 17–55, 17–37, 23–37, 25–29, and 33–35 from bAE1, respectively. Conversely, the chimeras bAE1/h[1–385], bAE1/h[18–39], and bAE1/h[26–30] contain the N-terminal amino acid residues 1–385, 18–39, and 26–30 of hAE1, respectively, in the corresponding regions of bAE1. The Δ11 mutants of these chimeras, in which the 11 C-terminal amino acid residues were deleted, were also prepared. hAE1 has a single *N*-glycosylation site on the fourth extracellular loop in the TM, whereas bAE1 does not (29). *B*, various bAE1-hAE1 chimeras and their Δ11 mutants were transfected into HEK293 cells, and their intracellular localizations were determined by confocal laser microscopy. EGFP fluorescence at the plasma membrane is indicated by *arrowheads*. *C*, HEK293 cells were transfected with EGFP-hAE1/b[25–29], EGFP-bAE1/h[26–30], and their Δ11 mutants. The cells were fixed at 48 h after transfection and stained with an anti-calnexin antibody. EGFP fluorescence at the cell surface is indicated by *arrowheads*. EGFP- (*green*), calnexin- (*red*), and DAPI-stained nuclei (*blue*) are shown in the merged images. *Bars*, 10 μm. *D*, cell surface expression of hAE1/b[25–29], bAE1/h[26–30], and their Δ11 mutants was examined by cell surface biotinylation as described in the legend for Fig. 1. AE1 proteins in the total (*Total*), intracellular (*Intracellular*), and cell surface (*Surface*) fractions were detected by immunoblotting using an anti-GFP antibody. The amount of cell surface fraction loaded is 10-fold higher than that of the other fractions. The migrating positions of the size markers are shown in kDa.

Confocal laser microscopy was performed as described previously (29, 30, 34). In some experiments, the images were analyzed using the co-localization function of LSM5 PASCAL software to obtain Pearson's correlation coefficients to estimate the degree of co-localization between two proteins in the region of interest.

Preparation of bN[1–37]-Halo and hN[1–39]-Halo—The bait polypeptide bN[1–37]-Halo, in which the N-terminal peptide of bovine AE1 was fused to the N terminus of the Halo tag, was generated and used to isolate interacting proteins. The cDNA for bN[1–37] and the cDNA fragment for the Halo tag from the pTH2 vector (Promega) were ligated into the pGEX-6P-1 vector using EcoRI, SalI, and NotI restriction sites. *Escherichia coli* BL21(DE3)pLyS competent cells (Promega) were transformed with the pGEX vector, and protein expression was induced with 1 mM isopropyl-β-thiogalactopyranoside for 6 h

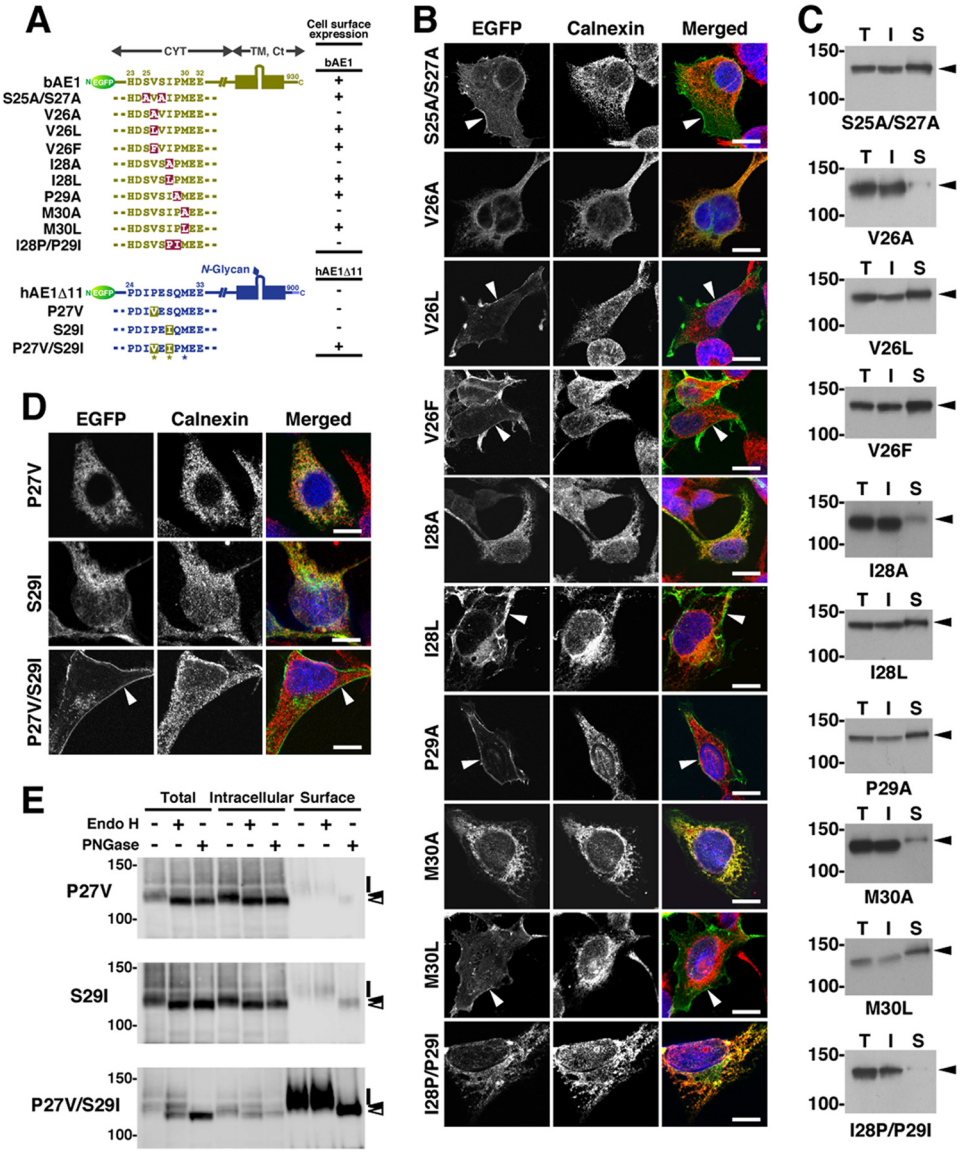

FIGURE 3. **Identification of the N-terminal amino acid sequence of AE1 required for its cell surface expression.** *A*, various amino acid substitution mutants of EGFP-bAE1 and EGFP-hAE1Δ11 were transfected into HEK293 cells. Mutated amino acid residues are highlighted. *B–D*, the cell surface expression of these mutants, as determined by laser confocal microscopy and cell surface biotinylation studies, are summarized by + and −, indicating positive and negative (less than 5% of the total amount) cell surface expression, respectively. *CYT*, *TM*, and *Ct* indicate the N-terminal cytoplasmic domain, the transmembrane domain, and the short cytoplasmic C-terminal tail, respectively. bAE1 is not *N*-glycosylated (29), whereas hAE1 possesses a single *N*-glycan in the extracellular loop. *B* and *C*, HEK293 cells were transfected with various EGFP-bAE1 mutants in which one or two amino acid residues in the ^{25}SVSIPM^{30} sequence were substituted by the indicated residue(s). After 48 h, the intracellular localizations of the mutants was analyzed by confocal laser microscopy (*B*) and cell surface biotinylation (*C*), as described in the legend of Fig. 1. In *B*, EGFP fluorescence at the plasma membrane is indicated by *arrowheads*. EGFP- (*green*), calnexin- (*red*), and DAPI-stained nuclei are shown in the merged images. *Bars*, 10 μm. In *C*, bAE1 mutants detected by immunoblotting of the total (*T*), intracellular (*I*), and cell surface (*S*) fractions are shown, and the migrating positions of the size markers are shown in kDa. Cell surface expression of each mutant was determined by the presence of EGFP fluorescence at the plasma membrane (*B*) and when the relative abundance of the mutant in the cell surface fraction comprised more than 5% of the total amount, as determined by densitometric scanning of the immunoblots (*C*). *D* and *E*, intracellular localization of hAE1Δ11/P27V, hAE1Δ11/S29I, and hAE1Δ11/P27V/S29I was examined by confocal laser microscopy (*D*) and cell surface biotinylation (*E*) as described in the legend to Fig. 1. EGFP fluorescence at the plasma membrane is indicated by *arrowheads* in *D*. Total (*Total*), intracellular (*Intracellular*), and cell surface (*Surface*) fractions were deglycosylated with endo H or peptide *N*-glycosidase F (*PNGase*). The amount of cell surface fraction loaded is 10-fold higher than that of the other fractions. *Symbols* indicate the migrating positions of each hAE1Δ11 mutant with mature and processed *N*-glycans (*bars*), endo H-sensitive immature *N*-glycans (*closed arrowheads*), and the deglycosylated polypeptides (*open arrowheads*). The migrating positions of the size markers are shown in kDa. *Bars*, 10 μm.

at 30 °C. Bacterial cells were collected by centrifugation and lysed in the B-PER reagent (Thermo Scientific). GST-fused bN[1–37] in the lysate was trapped on glutathione-Sepharose beads (Amersham Biosciences). Finally, bN[1–37]-Halo was cleaved from GST by the addition of Turbo 3C protease (Wako Pure Chemical Industries, Osaka, Japan) and eluted from the beads. hN[1–39]-Halo was generated using the same procedure.

Isolation and Identification of Proteins That Interact with the N Terminus of Bovine AE1 by Fourier Transform-MS/MS Analysis—Affinity isolation of the cellular interacting proteins was performed according to the procedure described previ-

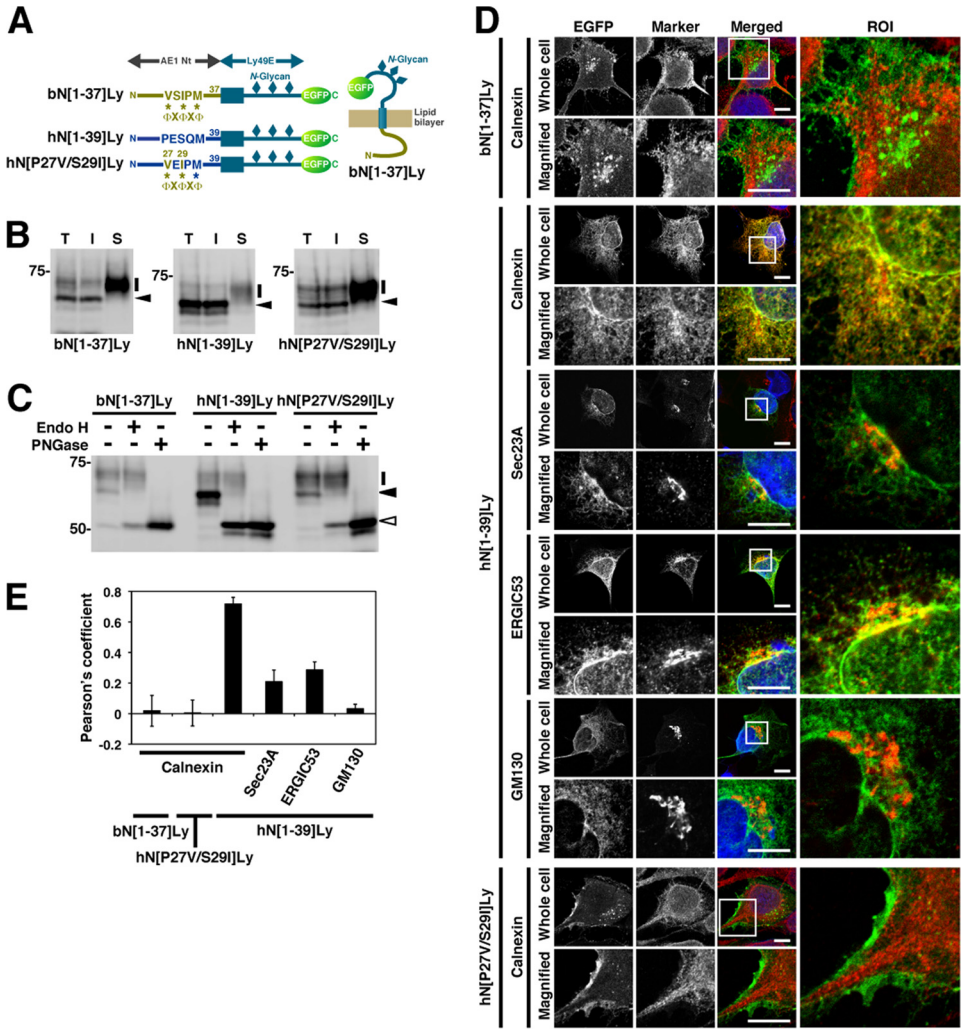

FIGURE 4. **Intracellular distribution of the AE1-Ly49E chimeric proteins.** *A*, schematic illustration of the AE1 N terminus-Ly49E chimeric proteins (bN[1–37]Ly, hN[1–39]Ly, and hN[P27V/S29I]Ly), which contain the N-terminal cytoplasmic regions (*AE1 Nt*) of bAE1, hAE, or hAE1/P27V/S29I and the transmembrane and extracellular domains of Ly49E with an N-terminal EGFP tag. *B–D*, AE1-Ly49E mutants were transfected into HEK293 cells, and their intracellular localizations were analyzed by biotinylation (*B*), deglycosylation (*C*), and confocal laser microscopy (*D*) as described in the legends to Figs. 1 and 2. A representative immunoblot of three independent experiments is presented in *B*. *T*, *I*, and *S* indicate the total, intracellular, and cell surface fractions, respectively. The amount of cell surface fraction loaded is 10-fold higher than that of the other fractions. In *B* and *C*, *bars*, *closed arrowheads*, and *open arrowheads* indicate the migrating positions of the mutant proteins whose *N*-glycan is endo H-resistant, endo H-sensitive, and deglycosylated, respectively. The migrating positions of the size markers are shown in kDa. In *D*, EGFP fluorescence (*green*) was visualized in HEK293 cells expressing bN[1–37]Ly, hN[1–39]Ly, or hN[P27V/S29I]Ly, and the ER, ER exit sites, ERGIC, and *cis*-Golgi were stained with anti-calnexin, anti-Sec23A, anti-ERGIC53, and anti-GM130 antibodies, respectively (*red*). Representative images are shown. The indicated areas of the region of interest (*ROI*) in the merged images are magnified (*Magnified*). *Bars*, 10 μm. *E*, Pearson's coefficients of co-localization between AE1-Ly49E chimeric proteins and organelle markers were analyzed. Co-localization was analyzed for each marker in the ROIs of 24 cells using LSM5 PASCAL co-localization software. The data are shown as the means ± S.D. ($n = 24$).

ously (13). In brief, HEK293 cells were homogenized in lysis buffer containing 50 mM Tris-Cl (pH 7.4), 0.5 mM EDTA, 1.3% (w/v) CHAPS, and 5 μg/ml aprotinin, 1 μg/ml leupeptin, 1 μg/ml pepstatin A, and 1 mM 4-(2-aminoethyl)-benzenesulfonyl fluoride (all from Sigma). The lysate was centrifuged for 1 h at 10,000 × *g* and the supernatant was incubated with gentle agitation for 16 h at 4 °C with bN[1–37]-Halo or hN[1–39]-Halo, which was immobilized on HaloLink resin (Promega). The resin was washed four times with lysis buffer containing 5 M NaCl and once with lysis buffer. Polypeptides bound to the resin were separated by SDS-PAGE on a 5–20% gradient gel (Wako Pure Chemical Industries) and stained with Coomassie Brilliant Blue. Polypeptides of interest were excised and subjected to reduction with dithiothreitol, alkylation with iodoacetamide, and digestion with trypsin Gold (Promega) according to the manufacturer's instructions. Tryptic peptides were separated and analyzed on a tandemly connected Dionex UltiMate 3000 liquid chromatography and LTQ Orbitrap Fourier transform-MS/MS system (Thermo Scientific). The MS/MS data were searched against the human database of the International Protein Index using the Proteome Discoverer 1.0 (Thermo Scientific).

Binding Assay for the Interaction of bN[1–37]-Halo with Sec24 Isoforms—The interaction of the bacterially produced bN[1–37]-Halo protein with Sec24 isoforms and Sec24C-AAA was principally analyzed as described above. Cell lysates from HEK293 cells expressing Myc-tagged Sec24A, Sec24B, Sec24C, Sec24D, or Sec24C-AAA were incubated with bN[1–37]-Halo

immobilized on the resin and processed as described above. Sec24 proteins bound to the resin were detected by immunoblotting using the anti-Myc antibody.

Statistical Analysis—Statistical significance was assessed using paired Student's *t* test.

RESULTS

Identification of the N-terminal Sequence of Bovine AE1 Required for Its Efficient Cell Surface Expression—A portion of human erythroid AE1 N-terminally tagged with EGFP (hAE1) was detected at the cell periphery, demonstrating its cell surface expression in transfected HEK293 cells (Fig. 1*B*). However, the C-terminal truncation mutant of hAE1 (hAE1Δ11) co-localized with calnexin, indicating that it was retained in the ER. When transfected into the same cell line, untagged hAE1 and hAE1Δ11 are reported to exhibit similar localizations to those of EGFP-hAE1 and EGFP-hAE1Δ11, respectively (28). This indicates that the N-terminal EGFP tag does not have a marked effect on the intracellular distribution of hAE1 or hAE1Δ11. By contrast, EGFP-bAE1Δ11 (bAE1Δ11) and its wild-type form (bAE1) were abundantly detected at the plasma membrane (Fig. 1*B*). Cell surface biotinylation showed that ~11% and less than 3% of hAE1 and hAE1Δ11 were detected at the cell surface, respectively, whereas ~11% of bAE1 and bAE1Δ11 were present at the cell surface (Fig. 1*C*), confirming our previous observations (30). These data indicate that a mechanism serves to deliver bAE1 to the cell surface, which is unaffected by the presence or absence of the 11 C-terminal amino acid residues.

We examined the intracellular localization of bAE1Δ11 and hAE1Δ11 chimeric proteins (Fig. 2*A*). The hAE1Δ11 chimera, whose N-terminal cytoplasmic domain was replaced with that of bAE1 (hAE1Δ11/b[1–403]), showed plasma membrane localization (Fig. 2*B*). By contrast, cell surface expression of bAE1Δ11 was markedly reduced by substitution of its cytoplasmic domain with that of hAE1, resulting in the retention of bAE1Δ11/h[1–385] in the ER. Thus, the key signal responsible for the plasma membrane targeting of bAE1 is present in the cytoplasmic domain. Subsequent microscopic and biotinylation studies on a series of chimeric AE1 proteins demonstrated that a portion of both hAE1/b[25–29] and its Δ11 mutant were expressed at the plasma membrane (Fig. 2, *C* and *D*). This demonstrates that replacement of the ^{26}IPESQ^{30} sequence with the corresponding ^{25}SVSIP^{29} bovine sequence is sufficient to facilitate effective targeting of hAE1 and hAE1Δ11 to the plasma membrane. This was further supported by the loss of cell surface expression and ER retardation of bAE1 and bAE1Δ11 when their ^{25}SVSIP^{29} sequence was replaced with ^{26}IPESQ^{30} (bAE1/h[26–30]; Fig. 2, *C* and *D*).

We next generated a series of mutants of bAE1 and hAE1Δ11 possessing substitutions of certain amino acid residues in ^{25}SVSIP^{29} and neighboring positions and examined their cell surface expression by microscopy and biotinylation (Fig. 3). Alanine substitution of Ser^{25}, Ser^{27}, or Pro^{29} had no effect on the plasma membrane expression of bAE1 (Fig. 3, *B* and *C*). Alanine substitution of Val^{26} and Ile^{28} resulted in the ER retention of these proteins, and they were no longer detected at the cell surface, whereas replacement of these residues with leucine or phenylalanine did not alter the localization. Similarly, substitution of Met^{30}, the C-terminal neighboring residue of ^{25}SVSIP^{29}, with alanine markedly reduced the surface expression of AE1, whereas substitution with leucine did not. Moreover, the protein was not detected at the cell surface following mutation of ^{28}IP^{29} to ^{28}PI^{29}.

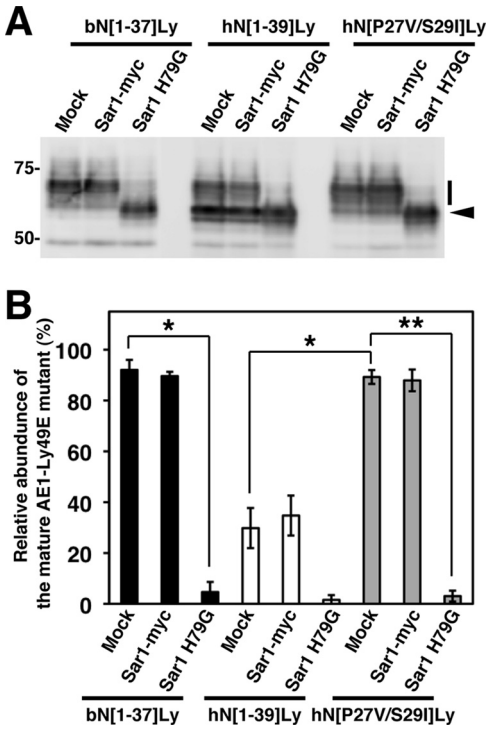

FIGURE 5. **Effect of Sar1A expression on the *N*-glycan processing of AE1-Ly49E reporter proteins.** *A*, HEK293 cells were co-transfected with a AE1-Ly49E mutant (*bN[1–37]Ly*, *hN[1–39]Ly*, or *hN[P29V/S29I]Ly*) and either an empty vector (*Mock*), C-terminally Myc-tagged Sar1A (*Sar1-myc*), or its activated form (*Sar1 H79G*). After 48 h of incubation, cell lysates were prepared, and AE1-Ly49E mutants were detected by immunoblotting with an anti-GFP antibody. A representative immunoblot from three independent experiments is presented. *Bars* and *arrowheads* indicate the migrating positions of AE1-Ly49E mutants with mature and immature *N*-glycans, respectively. The migrating positions of the size markers are shown in kDa. *B*, the abundance of the AE1-Ly49E mutants bearing mature *N*-glycans relative to the total amount was quantitated by densitometric scanning of the immunoblots. The data are expressed as the means ± S.D. ($n = 3$). *, $p < 0.05$; **, $p < 0.005$.

Similarly, the cell surface expression of hAE1Δ11/P27V/S29I, in which the Pro^{27} and Ser^{29} residues of ^{26}IPESQ^{30} were mutated to valine and isoleucine, respectively, was markedly increased compared with that of hAE1Δ11, whereas no effect was observed when either of these residues was mutated individually (Fig. 3*D*). The intracellular fractions of hAE1Δ11/P27V and hAE1Δ11/S29I were sensitive to digestion with endo H (Fig. 3*E*), confirming their ER localization as indicated by co-localization with calnexin (Fig. 3*D*). By contrast, the cell surface fraction of hAE1Δ11/P27V/S29I was resistant to endo H, demonstrating its targeting to the plasma membrane through the Golgi apparatus, although a small portion of the intracellular fraction of this mutant was sensitive to endo H (Fig. 3*E*). These data demonstrate that the (V/L/F)*X*(I/L)*X*(M/L) sequence (^{26}VSIPM^{30} in bovine AE1) at this position, which corresponds to a Φ*X*Φ*X*Φ sequence, facilitates the plasma membrane targeting of AE1 and AE1Δ11, and suggests that this motif increases the ER-Golgi transport of these proteins.

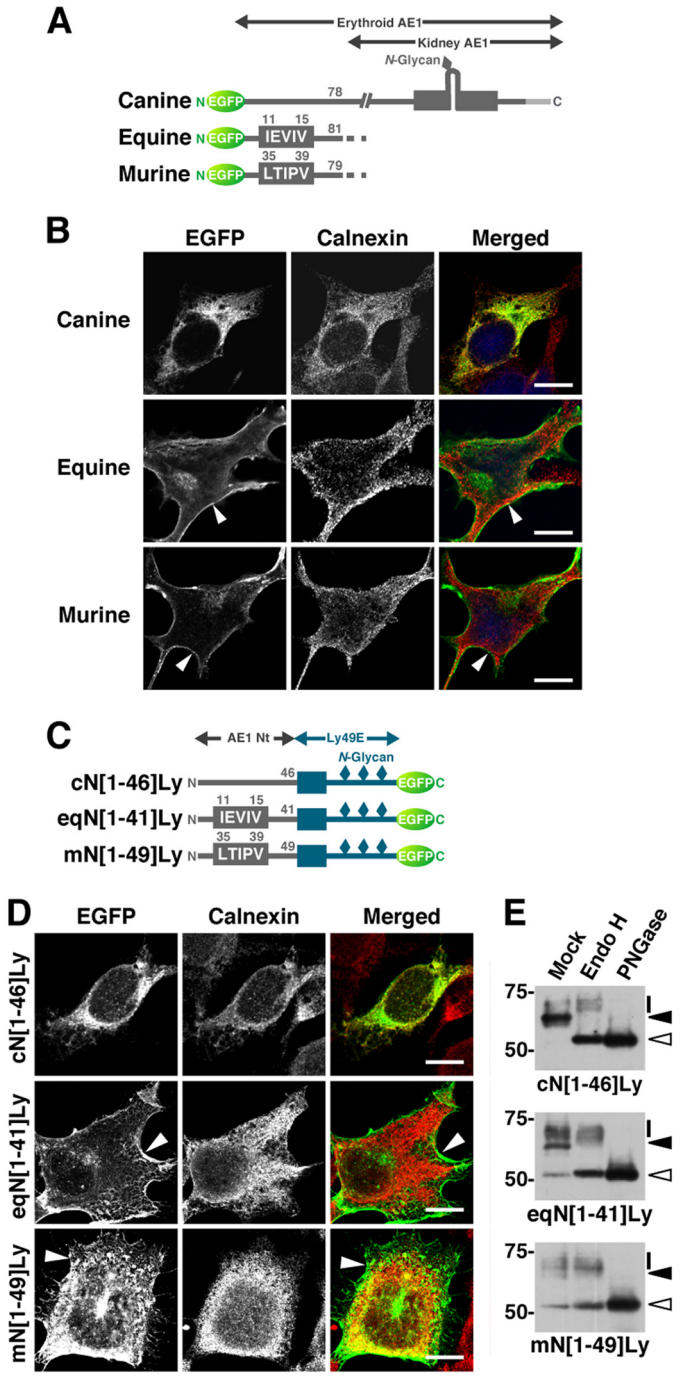

FIGURE 6. **Roles of the N-terminal sequences of erythroid AE1 from several species in the *N*-glycan processing and cell surface expression of the protein.** *A*, schematic illustration of EGFP-tagged AE1Δ11 mutants of canine, equine, and murine erythroid AE1. Equine and murine erythroid AE1 contain the N-terminal sequences ^{11}IEVIV^{15} and ^{35}LTIPV^{39}, which conform to the ΦXΦXΦ motif, respectively, whereas canine erythroid AE1 does not contain this motif as shown in Fig. 1*A*. *B*, EGFP-AE1Δ11 mutants described above were transfected into HEK293 cells, which were then fixed and stained for calnexin. Equine and murine AE1Δ11 were abundant at the plasma membrane (*arrowheads*), whereas canine AE1Δ11 exhibited a similar pattern to calnexin. EGFP- (*green*), calnexin- (*red*), and DAPI-stained nuclei (*blue*) are shown in the merged images. *C*, the partial sequences of the N-terminal regions of canine, equine, and murine erythroid AE1 (*AE1 Nt*) were substituted for the N-terminal cytoplasmic region of Ly49E to create the AE1-Ly49E chimeric proteins cN[1–46]Ly, eqN[1–41]Ly, and mN[1–49]Ly, respectively. *D* and *E*, HEK293 cells were transfected with cN[1–46]Ly, eqN[1–41]Ly, and mN[1–49]Ly and incubated for 48 h. The intracellular localization of the mutants was examined by confocal laser microscopy after staining with an anti-calnexin antibody (*D*), and *N*-glycan processing was analyzed by deglycosylation as described in the legends to Figs. 2 and 3 (*E*). In *D*, the plasma membrane expression of eqN[1–41]Ly and mN[1–49]Ly is indicated by *arrowheads*. *Bars*, 10 μm. In *E*, total cell lysates from the transfected cells were mock treated, endo H-treated, or peptide *N*-glycosidase F (*PNGase*)-treated and then immunoblotted with an anti-EGFP antibody. The migrating positions of each AE1-Ly49E mutant with mature and processed *N*-glycans (*bars*), endo H-sensitive immature *N*-glycans (*closed arrowheads*), and the deglycosylated polypeptides (*open arrowheads*) are indicated. The migrating positions of the size markers are shown in kDa.

Identification of the ΦXΦXΦ Sequence as an ER Export Signal—To verify this hypothesis, we first examined whether the insertion of the ΦXΦXΦ sequence was sufficient to induce the plasma membrane targeting of another protein. For this purpose, we used Ly49E, a type II transmembrane protein consisting of a short cytoplasmic N terminus, a single transmembrane α-helix, and a large extracellular C-terminal lectin-like domain (31, 32), as a reporter protein. Three potential *N*-glycosylation sites in Ly49E meant different forms of the protein with mature processed *N*-glycan or with immature core *N*-glycan could be distinguished. The redistribution of Ly49E has been monitored following replacement of its N terminus with that of the human CLC-4 chloride channel (35).

We created reporter proteins containing the Ly49E backbone and a C-terminal EGFP tag, namely bN[1–37]Ly, hN[1–39]Ly, and hN[P27V/P29I]Ly, whose N-terminal cytoplasmic regions were replaced by the N-terminal 1–37 residues of bAE1, residues 1–39 of hAE1, or residues 1–39 of hAE1 containing the P27V/P29I mutation, respectively (Fig. 4*A*). Approximately 17 and 18% of the total amount of bN[1–37]Ly and hN[P27V/S29I]Ly expressed in HEK293 cells was biotinylated at the cell surface, respectively, and they principally consisted of polypeptides of 63–73 kDa (Fig. 4*B*) whose *N*-glycan was resistant to endo H (Fig. 4*C*). By contrast, the vast majority of hN[1–39]Ly was 60 kDa in size, intracellular, and completely sensitive to endo H digestion. Microscopic analysis showed that bN[1–37]Ly and hN[P27V/S29I]Ly were localized at the plasma membrane with some juxtanuclear signals, whereas hN[1–39]Ly exhibited a reticular pattern that was consistent with calnexin (Fig. 4, *D* and *E*). hN[1–39]Ly partially co-localized with Sec23A and ERGIC53, which are markers of ER exit sites and the ERGIC, respectively, in juxtanuclear areas, but did not co-localize with GM130, a marker of the *cis*-Golgi.

An activated form of Sar1A, Sar1A H79G, inhibits the formation of COPII-coated vesicles (33). We analyzed the effect of Sar1A H79G on the *N*-glycan processing of AE1-Ly49E mutants (Fig. 5). Co-expression of Myc-tagged wild-type Sar1A had no significant effect on the relative abundance of bN[1–37]Ly, hN[1–39]Ly, or hN[P27V/S29I]Ly with mature *N*-glycan, although the value for hN[1–39]Ly (17 ± 4%, $n = 3$) was much lower than that for bN[1–37]Ly (74 ± 4%, $n = 3$) and hN[P27V/S29I]Ly (68 ± 4%, $n = 3$). However, when Sar1A H79G was co-transfected, the relative abundance of the mature forms of bN[1–37]Ly and hN[P27V/S29I]Ly was markedly reduced to less than 5% of the total amount. This indicates that bN[1–37]Ly and hN[P27V/S29I]Ly were transported to the cell surface via the conventional secretory pathway.

These data demonstrate that the N-terminal segments bN[1–37] and hN[P27V/S29I] can induce effective ER export of the Ly49E reporters through the COPII pathway and that the

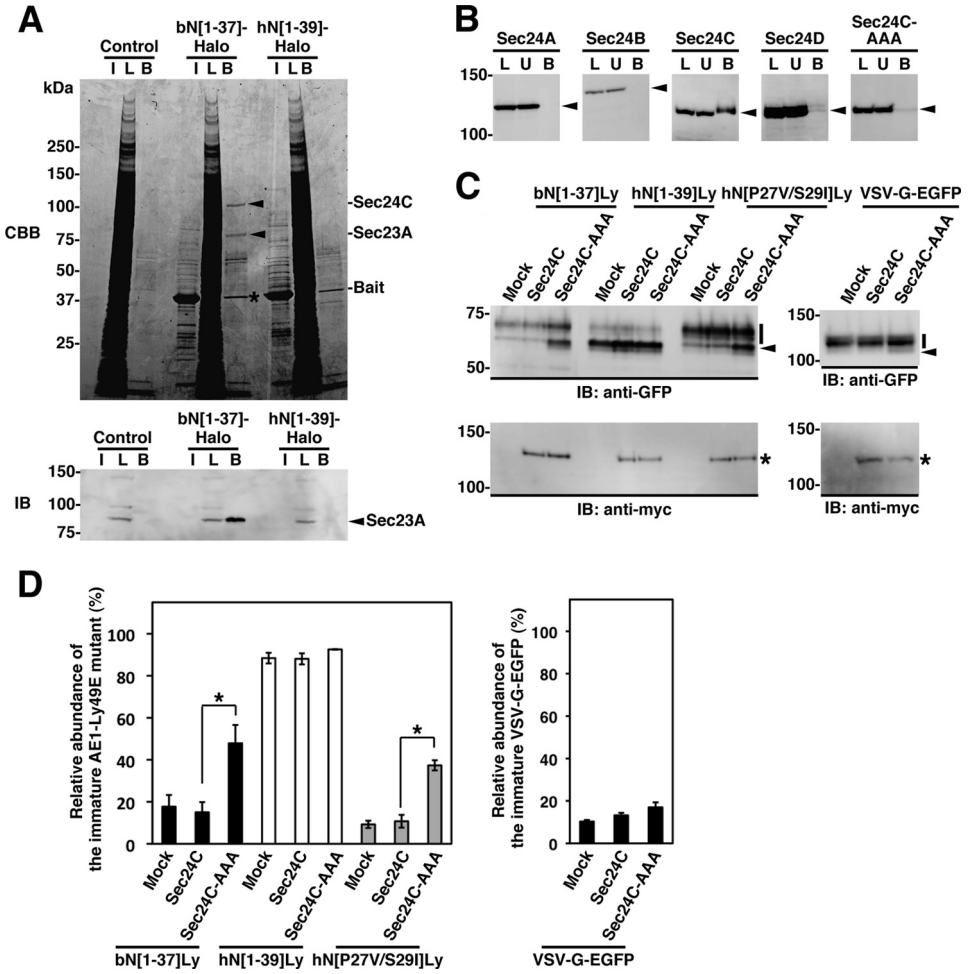

FIGURE 7. **Selective interaction between the ΦXΦXΦ motif and Sec24C.** *A*, HEK293 cell lysate (*lane L*) was incubated with bacterially expressed bN[1–37]-Halo or hN[1–39]-Halo protein that was immobilized on HaloLink resin or with the resin alone (*Control*). Bound proteins (*lane B*) were separated by SDS-PAGE on a 5–20% gradient gel followed by staining with Coomassie Brilliant Blue (*CBB*). The 120- and 85-kDa polypeptides that specifically bound to bN[1–37] were subjected to MS/MS analysis and were identified as Sec24C and Sec23A, respectively (indicated by *arrowheads*). *Lane I* contains the bait protein, and the *asterisk* indicates the bait protein that leaked from the resin. Immunoblotting (*IB*) with an anti-Sec23A antibody detected a band specifically in the fraction that bound the bN[1–37]-Halo-coupled resin and in the total cell lysate, which migrated at a size comparable with that of the 85-kDa protein (*lower panel*). Proteins in each fraction were separated on an 8% gel and were immunoblotted. *B*, lysates from HEK293 cells expressing Myc-tagged Sec24 isoforms (*Sec24A*, *Sec24B*, *Sec24C*, and *Sec24D*) or Sec24C-AAA were incubated with bN[1–37]-Halo-coupled resin as described above. Sec24 proteins in cell lysates (*L*), unbound (*U*), and bound (*B*) fractions were detected by immunoblotting with an anti-Myc antibody (indicated by *arrowheads*). *C* and *D*, the effect of Sec24C-AAA on *N*-glycan processing of AE1-Ly49E chimeric proteins was examined. HEK293 cells were co-transfected with an AE1-Ly49E mutant (*bN[1–37]Ly*, *hN[1–39]Ly*, or *hN[P27V/S29I]Ly*) or VSV-G-EGFP and either the empty vector (*Mock*), Myc-tagged Sec24C (*Sec24C*), or its Sec24C-AAA mutant (*Sec24C-AAA*). After 48 h, the AE1-Ly49E and VSV-G proteins and Sec24C proteins in the cell lysates were detected by immunoblotting with anti-GFP and anti-Myc antibodies, respectively. Representative immunoblots from three independent experiments are shown in *C*. The migrating positions of AE1-Ly49E mutants and VSV-G with mature and immature *N*-glycans are indicated by a *bar* and an *arrowhead*, respectively. The *asterisk* indicates Sec24C proteins. The migrating positions of the size markers are shown in kDa. *D*, the abundance of AE1-Ly49E and VSV-G proteins with mature and immature *N*-glycans relative to the total amount were quantitated by densitometric scanning of the immunoblots. The data are expressed as the means ± S.D. ($n = 3$). *, $p < 0.05$; **, $p < 0.005$.

P27V/S29I substitution, *i.e.*, creation of the ΦXΦXΦ motif, significantly increased the basal level of hN[1–39]Ly ER exit. Therefore, we next tested whether hydrophobic clusters of AE1 proteins from several other species that contain a ΦXΦXΦ motif behave as the bovine sequence does. When transfected into HEK293 cells, equine and murine AE1Δ11 mutants that contain ^{11}IEVIV^{15} and ^{35}LTIPV^{39} in the N-terminal stretches, respectively, were found at the plasma membrane, whereas canine AE1Δ11, which lacks an N-terminal ΦXΦXΦ sequence, was retained in the ER (Fig. 6, *A* and *B*; also see Fig. 1*A*). Moreover, chimeras containing the first 41 or 49 amino acids of equine or murine AE1, respectively, and the transmembrane and C-terminal regions of Ly49E exhibited effective cell surface expression and endo H-resistant *N*-glycans, whereas a chimera possessing the 46 N-terminal residues of canine AE1 was primarily unprocessed and was not detected at the cell surface (Fig. 6, *C–E*). Based on these findings, we conclude that the ΦXΦXΦ motif facilitates the ER export of membrane proteins.

Selective Interaction of the ΦXΦXΦ Motif with Sec24C—These findings suggest that some COPII components, or other adaptor proteins, interact with the ΦXΦXΦ sequence upon ER exit. To identify the interacting protein(s), we isolated proteins that specifically bound to the motif from HEK293 cell lysates using bN[1–37]-Halo tag fusion proteins as the bait. Two polypeptides of 120 and 85 kDa were identified, which bound to bN[1–37]-Halo, but not to hN[1–39]-Halo (Fig. 7*A*). MS/MS analysis of these bands and a database search identified the 120- and 85-kDa proteins as human Sec24C and Sec23A, respec-

tively (supplemental Table S2). Moreover, the 85-kDa polypeptide reacted specifically with an anti-Sec23A antibody on immunoblots (Fig. 7*A*, *lower panel*). In the Sec23-Sec24 complex, Sec24 is the primary cargo selection element (1, 9, 10), and two mammalian paralogues of Sec23, Sec23A and Sec23B, serve distinct functions, probably because of their differential tissue-specific expression (16). Therefore, we hereafter focus on Sec24C in this study.

Using the same procedure, we tested the interaction between bN[1–37]-Halo and Myc-tagged Sec24A, Sec24B, Sec24C, or Sec24D by overexpressing these proteins in HEK293 cells to determine the specificity of bN[1–37]-Halo for the Sec24 isoforms. Sec24C bound to bN[1–37], whereas the other isoforms did not. In addition, the Sec24C-AAA mutant, in which the ^{895}LIL^{897} sequence that forms the binding pocket for the L*X*M motif on membrin and syntaxin 5 (11) was changed to ^{895}AAA^{897}, did not bind bN[1–37] (Fig. 7*B*). Furthermore, when the Sec24C-AAA mutant was co-transfected with the AE1-Ly49E chimeras, the abundance of the immature forms of bN[1–37] and hN[P27V/S29I] relative to the total amount was significantly higher than when they were mock co-transfected. By contrast, co-transfection of the Sec24C-AAA mutant caused no significant change in the abundance of the immature form of VSV-G, which interacts with Sec24A-Sec24B (4) (Fig. 7, *C* and *D*). There was no marked change in the relative abundance of the immature form of the chimeras in cells expressing wild-type Sec24C compared with that in mock treated cells (Fig. 7, *C* and *D*). Thus, the presence of Sec24C-AAA reduced the ER export of bN[1–37]Ly and hN[P27V/S29I]Ly, which both contain the Φ*X*Φ*X*Φ motif, indicating that the motif interacts with this region of Sec24C. These findings demonstrate that the Φ*X*Φ*X*Φ motif interacts with the Sec23A-Sec24C complex by specifically binding to ^{895}LIL^{897} on the surface of Sec24C and that this interaction potently increases the efficiency of ER export of cargo proteins.

DISCUSSION

The present study identified the Φ*X*Φ*X*Φ sequence as a new class of sorting signal that facilitates the ER export of cargo proteins through the COPII pathway. Various bovine and human AE1 mutants and Ly49E-based reporter proteins possessing a Φ*X*Φ*X*Φ motif were targeted to the cell surface with efficient *N*-glycan processing, whereas mutants and reporter proteins lacking this motif were largely retained in the ER (Figs. 1–4). The facilitation of ER export by the Φ*X*Φ*X*Φ motif was also verified by its selective binding to the Sec23A-Sec24C complex (Fig. 7). It is conceivable that the Φ*X*Φ*X*Φ motif acts as the primary signal for the ER export of cargo proteins and that a signal in the N terminus that facilitates the plasma membrane targeting of erythroid AE1 is present in specific species, including cattle, horse, and mouse.

Perhaps the most novel findings of the present study are that the Φ*X*Φ*X*Φ motif selectively interacts with Sec24C and that the motif appears to share the binding site on Sec24C with the L*X*M signal. The Sec24C-AAA mutant, in which the binding site sequence ^{895}LIL^{897} of the L*X*M motif (11) was mutated to ^{895}AAA^{897}, no longer interacted with AE1-Ly49E reporter proteins, resulting in their ER retention (Fig. 7). The Φ*X*Φ*X*Φ motif sequence ^{26}VSIPM^{30} in bovine AE1 includes ^{28}IPM^{30}, which is comparable with the L*X*M class ER export signal of membrin and syntaxin 5 (11). Conversely, the L*X*M motif and the sequence upstream of this motif in mammalian syntaxin 5 consists of V*X*L*X*M (^{189}VAIDM^{193} in the human sequence), which is comparable with the Φ*X*Φ*X*Φ sequence. However, these two motifs differ from each other in the following respects. First, although the L*X*M motif binds in the surface groove of Sec24C and Sec24D (11), the Φ*X*Φ*X*Φ motif specifically binds to Sec24C but not to Sec24D (Fig. 7). Second, creation of the ^{29}IQM^{31} sequence in hAE1Δ11 (hAE1Δ11/S29I) resulted in ER retention of the protein, and the coordinate mutation of Pro^{27} to generate the ^{27}VEIQM^{31} sequence (hAE1Δ11/P27V/S29I) was needed for efficient *N*-glycan processing and cell surface expression (Fig. 3). Therefore, the selective interaction between the Φ*X*Φ*X*Φ motif and Sec24 is likely due to structural differences between Sec24C and Sec24D in the region adjacent to the binding site with the LIL sequence, as well as to the structure of the motif on the cargo. Sec24C or Sec24D are absolutely required for binding the RI/RL motif of the highly related SLC6 family transporters (12, 13). The serotonin transporter SERT and the GABA transporter GAT1 interact with Sec24C and Sec24D, respectively, although both transporters bind to the relevant DD sequence on Sec24C-Sec24D machineries (12, 13).

As demonstrated by the previous structural analyses of the cytoplasmic domain of human erythroid AE1, a large part of the N-terminal stretch (the first 54 residues in human AE1 corresponding to residues 1–64 in bovine AE1 containing the ^{26}VSIPM^{30} sequence) is flexible and dynamically disordered (36, 37). When AE1 forms tetramers in the membrane, two of the N-terminal regions on the distal monomers in the tetramer that are not involved in the association with the bridging protein ankyrin are anticipated to be in close proximity to the lipid bilayer (36). On the other hand, the common binding pocket for the Φ*X*Φ*X*Φ and L*X*M motifs containing the ^{895}LIL^{897} sequence in the distal region of Sec24C in the Sec23-Sec24-Sar1 complex faces toward and is in close proximity to the membrane (2, 11, 38). Therefore, it is likely that the interaction of the AE1 Φ*X*Φ*X*Φ motif with Sec24C readily occurs on the surface close to the ER membrane. AE1 exists primarily as a mixture of dimers and tetramers in membranes (39), and AE1 forms a dimer in the ER (29). Binding of ankyrin induces two dimers to form a tetramer (39, 40), and this AE1-ankyrin interaction occurs in the ER when both proteins are exogenously expressed (41, 42). These findings indicate that AE1 is present as a dimer and forms a tetramer in the ER when ankyrin is available. Hence, the interaction between the Φ*X*Φ*X*Φ motif and Sec24C may contribute to cooperative incorporation and concentration of AE1, ankyrin, and the COPII machineries into prebudding vesicles.

Our observations on the N-terminal ER export signal do not rule out the possibility that an unidentified signal(s) also participates in the plasma membrane targeting of AE1. Indeed human and canine AE1, which do not have a Φ*X*Φ*X*Φ motif in the N terminus, are transported to the plasma membrane in red blood cells. In fact, cell surface biotinylation and *N*-glycan maturation of AE1 mutants and AE1-Ly49E mutants lacking this motif (*e.g.*, hAE1Δ11 and hN[1–39]Ly, etc.; Figs. 1, 4, and 5) were detected,

although at much lower efficiency than those of proteins bearing the Φ*X*Φ*X*Φ motif. A marked fraction of hN[1–39]Ly containing the first 39 residues of human AE1 exited the ER (Fig. 4), and this region has no known ER export signal, except for several diacidic sequences representing the (D/E)*X*(D/E) motif; therefore, any of these diacidic residues are candidate ER exit signals for erythroid AE1 in various species including humans (Fig. 1*A*). The highly conserved EL*XX*L(D/E) (^{882}ELQCLD^{887} in human AE1) in the C-terminal region is another candidate signal. This sequence is essential for the proper targeting of erythroid AE1 to the cell surface in HEK293 cells (30) and matches the L*XX*LE class of ER export signal found in the yeast SNARE protein Bet1 (9, 10). Diacidic and L*XX*LE motifs share the same binding site on mammalian Sec24A and Sec24B (11, 15, 16).

We do not have a rational explanation for why the sequences of ER export signals of AE1 exhibit such variability in mammals. However, such sequence variability might occur in many proteins, and different signal motifs might be used in different contexts or be part of a compensatory mechanism for the intracellular trafficking of a single protein species. For example, we are intrigued by the possible use of distinct signal motifs in different mammals for the interaction between neutrophil lysosomal elastase and the AP-3 adaptor protein complex. Mutations in the *AP3B1* gene, which encodes the β subunit of AP-3, are responsible for cyclic neutropenia, which is associated with a deficiency of neutrophil elastase (ELA2), in humans and dogs (43). However, the tyrosine-based signal in human ELA2, which interacts with AP-3 (43), is not conserved in canine ELA2 (GenBank^{TM} accession number AF494190). This suggests that a different signal motif, such as a dileucine signal that is recognized by AP-3 (44), is used to target ELA2 to lysosomes in dogs. Moreover, clathrin-mediated endocytosis of bovine AE1 uses a noncanonical Y*XXX*Φ motif instead of the Y*XX*Φ signal (34), and this is another example of variability in the sequences of motifs used for cargo recognition.

In conclusion, we demonstrate that a novel Φ*X*Φ*X*Φ sequence functions as an ER export signal through selective binding to the prebudding complex component Sec24C. Elucidation of the mechanism responsible for the Φ*X*Φ*X*Φ motif-Sec24C interaction and the cargo molecules that utilize this interaction to exit the ER may shed further light on the mechanisms underlying intracellular trafficking of membrane and secretory proteins and on the etiology of diseases that are caused by impaired trafficking.

REFERENCES

1. Bonifacino, J. S., and Glick, B. S. (2004) The mechanisms of vesicle budding and fusion. *Cell* **116,** 153–166
2. Mancias, J. D., and Goldberg, J. (2005) Exiting the endoplasmic reticulum. *Traffic* **6,** 278–285
3. Mellman, I., and Nelson, W. J. (2008) Coordinated protein sorting, targeting and distribution in polarized cells. *Nat. Rev. Mol. Cell Biol.* **9,** 833–845
4. Nishimura, N., and Balch, W. E. (1997) A di-acidic signal required for selective export from the endoplasmic reticulum. *Science* **277,** 556–558
5. Wang, X., Matteson, J., An, Y., Moyer, B., Yoo, J.-S., Bannykh, S., Wilson, I. A., Riordan, J. R., and Balch, W. E. (2004) COPII-dependent export of cystic fibrosis transmembrane conductance regulator from the ER uses a di-acidic exit code. *J. Cell Biol.* **167,** 65–74
6. Ma, D., Zerangue, N., Lin, Y.-F., Collins, A., Yu, M., Jan, Y. N., and Jan, L. Y. (2001) Role of ER export signals in controlling surface potassium channel numbers. *Science* **291,** 316–319
7. Nufer, O., Guldbrandsen, S., Degen, M., Kappeler, F., Paccaud, J.-P., Tani, K., and Hauri, H.-P. (2002) Role of cytoplasmic C-terminal amino acids of membrane proteins in ER export. *J. Cell Sci.* **115,** 619–628
8. Nufer, O., Kappeler, F., Guldbrandsen, S., and Hauri, H.-P. (2003) ER export of ERGIC-53 is controlled by cooperation of targeting determinants in all three of its dominants. *J. Cell Sci.* **116,** 4429–4440
9. Miller, E. A., Beilharz, T. H., Malkus, P. N., Lee, M. C., Hamamoto, S., Orci, L., and Schekman, R. (2003) Multiple cargo binding sites on the COPII subunit Sec24p ensure capture of diverse membrane proteins into transport vesicles. *Cell* **114,** 497–509
10. Mossessova, E., Bickford, L. C., and Goldberg, J. (2003) SNARE selectivity of the COPII coat. *Cell* **114,** 483–495
11. Mancias, J. D., and Goldberg, J. (2008) Structural basis of cargo membrane protein discrimination by the human COPII coat machinery. *EMBO J.* **27,** 2918–2928
12. Farhan, H., Reiterer, V., Korkhov, V. M., Schmid, J. A., Freissmuth, M., and Sitte, H. H. (2007) Concntrative export from the endoplasmic reticulum of the γ-aminobutyric acid transporter 1 requires binding to SEC24D. *J. Biol. Chem.* **282,** 7679–7689
13. Sucic, S., El-Kasaby, A., Kudlacek, O., Sarker, S., Sitte, H. H., Marin, P., and Freissmuth, M. (2011) The serotonin transporter is an exclusive client of the coat protein complex II (COPII) component SEC24C. *J. Biol. Chem.* **286,** 16482–16490
14. Gillon, A. D., Latham, C. F., and Miller, E. A. (2012) Vesicle-mediated ER export of proteins and lipids. *Biochim. Biophys. Acta* **1821,** 1040–1049
15. Russell, C., and Stagg, S. M. (2010) New insights into the structural mechanisms of the COPII coat. *Traffic* **11,** 303–310
16. Zanetti, G., Pahuja, K. B., Studer, S., Shim, S., and Schekman, R. (2012) COPII and the regulation of protein sorting in mammals. *Nat. Cell Biol.* **14,** 20–28
17. Wendeler, M. W., Paccaud, J.-P., and Hauri, H.-P. (2007) Role of Sec24 isoforms in selective export of membrane proteins from the endoplasmic reticulum. *EMBO Rep.* **8,** 258–264
18. Khoriaty, R., Vasievich, M. P., and Ginsburg, D. (2012) The COPII pathway and hematologic disease. *Blood* **120,** 31–38
19. Tzetis, M., Efthymiadou, A., Strofalis, S., Psychou, P., Dimakou, A., Pouliou, E., Doudounakis, S., and Kanavakis, E. (2001) CFTR gene mutations—including three novel nucleotide substitutions—and haplotype background in patients with asthma, disseminated bronchiectasis and chronic obstructive pulmonary disease. *Hum. Genet.* **108,** 216–221
20. Tanner, M. J. (2002) Band 3 anion exchanger and its involvement in erythrocyte and kidney disorders. *Curr. Opin. Hematol.* **9,** 133–139
21. Alper, S. L. (2006) Molecular physiology of SLC4 anion exchangers. *Exp. Physiol.* **91,** 153–161
22. Inaba, M., Yawata, A., Koshino, I., Sato, K., Takeuchi, M., Takakuwa, Y., Manno, S., Yawata, Y., Kanzaki, A., Sakai, J., Ban, A.,Ono, K., and Maede, Y. (1996) Defective anion transport and marked spherocytosis with membrane instability caused by hereditary total deficiency of red cell band 3 in cattle due to a nonsense mutation. *J. Clin. Invest.* **97,** 1804–1817
23. Yenchitsomanus, P.-T., Kittanakom, S., Rungroj, N., Cordat, E., and Reithmeier, R. A. (2005) Molecular mechanisms of autosomal dominant and recessive distal renal tubular acidosis caused by SLC4A1 (AE1) mutations. *J. Mol. Genet. Med.* **1,** 49–62
24. Devonald, M. A., Smith, A. N., Poon, J. P., Ihrke, G., and Karet, F. E. (2003) Non-polarized targeting of AE1 causes autosomal dominant distal renal tubular acidosis. *Nat. Genet.* **33,** 125–127
25. Toye, A. M., Banting, G., and Tanner, M. J. (2004) Regions of human kidney anion exchanger 1 (kAE1) required for basolateral targeting of kAE1 in polarised kidney cells. Mis-targeting explains dominant renal tubular acidosis (dRTA). *J. Cell Sci.* **117,** 1399–1410
26. Williamson, R. C., Brown, A. C., Mawby, W. J., and Toye, A. M. (2008) Human kidney anion exchanger 1 localization in MDCK cells is controlled by the phosphorylation status of two critical tyrosines. *J. Cell Sci.* **121,** 3422–34432
27. Toye, A. M., Bruce, L. J., Unwin, R. J., Wrong, O., and Tanner, M. J. (2002) Band 3 Walton, a C-terminal deletion associated with distal renal tubular

acidosis, is expressed in the red cell membrane but retained internally in kidney cells. *Blood* **99,** 342–347
28. Quilty, J. A., Cordat, E., and Reithmeier, R. A. (2002) Impaired trafficking of human kidney anion exchanger (kAE1) caused by hetero-oligomer formation with a truncated mutant associated with distal renal tubular acidosis. *Biochem. J.* **368,** 895–903
29. Ito, D., Koshino, I., Arashiki, N., Adachi, H., Tomihari, M., Tamahara, S., Kurogi, K., Amano, T., Ono, K., and Inaba, M. (2006) Ubiquitylation-independent ER-associated degradation of an AE1 mutant associated with dominant hereditary spherocytosis in cattle. *J. Cell Sci.* **119,** 3602–3612
30. Adachi, H., Ito, D., Kurooka, T., Otsuka, Y., Arashiki, N., Sato, K., and Inaba, M. (2009) Structural implications of the EL(K/Q)(L/C)LD(A/G)DD sequence in the C-terminal cytoplasmic tail for proper targeting of anion exchanger 1 to the plasma membrane. *Jpn. J. Vet. Res.* **57,** 135–146
31. Van Beneden, K., Stevenaert, F., De Creus, A., Debacker, V., De Boever, J., Plum, J., and Leclercq, G. (2001) Expression of Ly49E and CD95/NKG2 on fetal and adult NK cells. *J. Immunol.* **166,** 4302–4311
32. Yokoyama, W. M., and Plougastel, B. F. (2003) Immune functions encoded by the natural killer gene complex. *Nat. Rev. Immunol.* **3,** 304–316
33. Aridor, M., Bannykh, S. I., Rowe, T., and Balch, W. E. (1995) Sequential coupling between COPII and COPI vesicle coats in endoplasmic reticulum to Golgi transport. *J. Cell Biol.* **131,** 875–893
34. Wang, C.-C., Sato, K., Otsuka, Y., Otsu, W., and Inaba, M. (2012) Clathrin-mediated endocytosis of mammalian erythroid AE1 anion exchanger facilitated by a Y*XX*Φ or a noncanonical Y*XXX*Φ motif in the N-terminal stretch. *J. Vet. Med. Sci.* **74,** 17–25
35. Okkenhaug, H., Weylandt, K.-H., Carmena, D., Wells, D. J., Higgins, C. F., and Sardini, A. (2006) The human ClC-4 protein, a member of the CLC chloride channel/transporter family, is localized to the edoplasmic reticulum by its N-terminus. *FASEB J.* **20,** 2390–2392
36. Zhang, D., Kiyatkin, A., Bolin, J. T., and Low, P. S. (2000) Crystallographic structure and functional interpretation of the cytoplasmic domain of erythrocyte membrane band 3. *Blood* **96,** 2925–2933
37. Zhou, Z., DeSensi, S. C., Stein, R. A., Brandon, S., Dixit, M., McArdle, E. J., Warren, E. M., Kroh, H. K., Song, L., Cobb, C. E., Hustedt, E. J., and Beth, A. H. (2005) Solution structure of the cytoplasmic domain of erythrocyte membrane band 3 determined by site-directed spin labeling. *Biochemistry* **44,** 15115–15128
38. Bi, X., Corpina, R. A., and Goldberg, J. (2002) Structure of the Sec23/24-Sar1 pre-budding complex of the COPII vesicle coat. *Nature* **419,** 271–277
39. Van Dort, H. M., Moriyama, R., and Low, P. S. (1998) Effect of band 3 subunit equilibrium on the kinetics and affinity of ankyrin binding to erythrocyte membrane vesicles. *J. Biol. Chem.* **273,** 14819–14826
40. Michaely, P., and Bennett, V. (1995) The ANK repeat of erythrocyte ankyrin from two distinct but cooperative binding sites for the erythrocyte anion exchanger. *J. Biol. Chem.* **270,** 22050–22057
41. Adachi, H., Kurooka, T., Otsu, W., and Inaba, M. (2010) The forced aggresome formation of a bovine anion exchanger 1 (AE1) mutant through association with ΔF508-cystic fibrosis transmembrane conductance-regulator upon proteasome inhibition in HEK293 cells. *Jpn. J. Vet. Res.* **58,** 101–110
42. Gomez, S., and Morgans, C. (1993) Interaction between band 3 and ankyrin begins in early compartments of the secretory pathway and is essential for band 3 processing. *J. Biol. Chem.* **268,** 19593–19597
43. Benson, K. F., Li, F.-Q., Person, R. E., Albani, D., Duan, Z., Wechsler, J., Meade-White, K., Williams, K., Acland, G. M., Niemeyer, G., Lothrop, C. D., and Horwitz, M. (2003) Mutations associated with neutropenia in dogs and humans disrupt intracellular transport of neutrophil elastase. *Nat. Genet.* **35,** 90–96
44. Horwitz, M., Benson, K. F., Duan, Z., Li, F.-Q., and Person, R. E. (2004) Hereditary neutropenia. Dogs explain human neutrophil elastase mutations. *Trends Mol. Med.* **10,** 163–170
45. Zhu, Q., Lee, D. W., and Casey, J. R. (2003) Novel topology in C-terminal region of the human plasma membrane anion exchanger, AE1. *J. Biol. Chem.* **278,** 3112–3120